NASA TECHNICAL NOTE

NASA TN D-8375
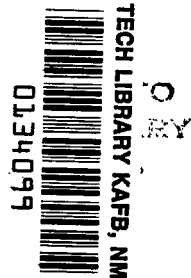
THREE-DIMENSIONAL POTENTIAL FLOW
OVER HILLS AND OVAL MOUNDS

Robert Siegel

Lewis Research Center
Cleveland, Ohio 44135

NATIONAL AERONAUTICS AND SPACE ADMINISTRATION • WASHINGTON, D. C. • DECEMBER 1976

1. Report No. NASA TN D-8375	2. Government Accession No.	3. Recipient's Catalog No.
4. Title and Subtitle THREE-DIMENSIONAL POTENTIAL FLOW OVER HILLS AND OVAL MOUNDS		5. Report Date December 1976
		6. Performing Organization Code
7. Author(s) Robert Siegel		8. Performing Organization Report No. E-8769
		10. Work Unit No. 506-24
9. Performing Organization Name and Address Lewis Research Center National Aeronautics and Space Administration Cleveland, Ohio 44135		11. Contract or Grant No.
12. Sponsoring Agency Name and Address National Aeronautics and Space Administration Washington, D.C. 20546		13. Type of Report and Period Covered Technical Note
		14. Sponsoring Agency Code

15. Supplementary Notes

16. Abstract

An analysis was made of the potential flow behavior for an initially uniform flow passing over a single axisymmetric hill, an oval mound, and a combination of two hills. Small perturbation theory was used, and the resulting Laplace equation for the perturbation velocity potential was solved by using either a product solution or a Green's function. The three-dimensional solution is of interest in calculating the pressure distribution around obstacles, the flow of pollutants carried by the wind, and the augmentation of wind velocity for windmill siting. The augmentation in velocity at the top of a hill was found to be proportional to the hill height relative to a characteristic width dimension of the hill. An axisymmetric hill produced about 20 percent less velocity increase than a two-dimensional ridge having the same cross-sectional profile.

17. Key Words (Suggested by Author(s)) Flow over topography Wind flow Three-dimensional flow Potential flow	18. Distribution Statement Unclassified - unlimited STAR Category 34	
19. Security Classif. (of this report) Unclassified	20. Security Classif. (of this page) Unclassified	21. No. of Pages 35	22. Price* $4.00

* For sale by the National Technical Information Service, Springfield, Virginia 22161

THREE-DIMENSIONAL POTENTIAL FLOW OVER HILLS AND OVAL MOUNDS

by Robert Siegel

Lewis Research Center

SUMMARY

An analysis was made of the potential flow behavior for an initially uniform flow passing over a single axisymmetric hill, an oval mound, and a combination of two hills. Small perturbation theory was used, and the resulting Laplace equation for the perturbation velocity potential was solved by using either a product solution or a Green's function. The three-dimensional solution is of interest in calculating the pressure distribution around obstacles, the flow of pollutants carried by the wind, and the augmentation of wind velocity for windmill siting. The augmentation in velocity at the top of a hill was found to be proportional to the hill height relative to a characteristic width dimension of the hill. An axisymmetric hill produced about 20 percent less velocity increase than a two-dimensional ridge having the same cross-sectional profile.

INTRODUCTION

The behavior of three-dimensional flow over irregular terrain is of interest for determining the flow path of pollutants, the pressure distribution over obstacles, and the augmentation of the wind velocity for selecting windmill sites. Some examples of air pollution studies are given by references 1 and 2, while reference 3 is related to wind utilization for power production.

With regard to wind utilization, the maximum power that can be extracted by a windmill depends on the cube of the wind velocity. Hence, in a location where there tend to be large steady winds, it would be of advantage to place a windmill such that the ground terrain will provide additional localized velocity increases. Possible locations would be at the top of a cliff or ridge facing the wind, the top of a circular or oval hill, or in the notch between two hills. Except for flow across a two-dimensional cliff or ridge, the prediction of the wind behavior involves three-dimensional calculations which are generally quite difficult.

A simplification that will allow some analytical results to be obtained is to consider

the flow to be inviscid. According to Sutton (ref. 4) the main features of the wind over the portion of a hill facing into the wind can be found from an inviscid solution. The inviscid results should provide a good indication of the relative effect on the flow of various types of terrain features. A small perturbation technique will be used to solve the inviscid relations, and this provides a limit on how steep the hills can be for the analysis to remain valid. For a two-dimensional ridge, all the flow must pass over the crest of the ridge. For a hill, however, some of the flow passes around the sides and thus provides what is called the three-dimensional relief effect. This effect reduces the maximum flow acceleration, and for the same terrain cross-sectional profile it causes the perturbation method to be more accurate for the three-dimensional case than for two dimensions (ref. 5).

In the perturbation theory the flow is determined by solving Laplace's equation for the velocity perturbation potential. Since this is a linear equation, superposition techniques can be used to build up solutions. Some solutions will be obtained by using the method employed by Scorer (refs. 6 and 7) wherein the flow is first obtained for a two-dimensional ridge. Then, results for oval mounds and circular hills can be obtained by superposing the ridges at various angles to the incident flow. Some solutions are also obtained by using Green's functions to solve the Laplace equation for the perturbation potential. The use of superposition also permits determining the effect of two adjacent hills as long as the second hill is not in a region where flow separation would be induced by the first hill thereby making the inviscid solution invalid.

ANALYSIS

Small Perturbation Equations

The flow across irregular terrain is idealized by assuming it to be incompressible and inviscid. The undisturbed flow is uniform and hence is irrotational; then, as a consequence of the inviscid assumption, the flow field remains irrotational everywhere. For irrotational flow the velocity components obey the relations

$$\left.\begin{aligned} \frac{\partial v}{\partial x} - \frac{\partial u}{\partial y} = 0 \\[2ex] \frac{\partial w}{\partial y} - \frac{\partial v}{\partial z} = 0 \\[2ex] \frac{\partial u}{\partial z} - \frac{\partial w}{\partial x} = 0 \end{aligned}\right\} \tag{1}$$

(All symbols are defined in appendix A.) These conditions are satisfied if there is a potential function Φ such that

$$
\left.
\begin{aligned}
u &= \frac{\partial \Phi}{\partial x} \\
\\
v &= \frac{\partial \Phi}{\partial y} \\
\\
w &= \frac{\partial \Phi}{\partial z}
\end{aligned}
\right\}
\tag{2}
$$

For steady incompressible flow the continuity equation is

$$
\frac{\partial u}{\partial x} + \frac{\partial v}{\partial y} + \frac{\partial w}{\partial z} = 0
\tag{3}
$$

Inserting equation (2) in equation (3) yields

$$
\frac{\partial^2 \Phi}{\partial x^2} + \frac{\partial^2 \Phi}{\partial y^2} + \frac{\partial^2 \Phi}{\partial z^2} = 0
\tag{4}
$$

so that the potential function is obtained by solving Laplace's equation.

The local variations in terrain height are assumed sufficiently small so that only small perturbations are produced on the incident uniform velocity. Then

$$
\left.
\begin{aligned}
u &= u_\infty + u' \\
\\
v &= v' \\
\\
w &= w'
\end{aligned}
\right\}
\tag{5}
$$

Let the velocity potential be

$$
\Phi(x, y, z) = u_\infty x + \varphi(x, y, z)
\tag{6}
$$

where $\varphi(x, y, z)$ is the perturbation potential such that

3

$$\frac{\partial \varphi}{\partial x} = u'$$

$$\frac{\partial \varphi}{\partial y} = v'$$

$$\frac{\partial \varphi}{\partial z} = w'$$

Substituting equation (6) into equation (4) shows that the perturbation potential also satisfies the Laplace equation

$$\frac{\partial^2 \varphi}{\partial x^2} + \frac{\partial^2 \varphi}{\partial y^2} + \frac{\partial^2 \varphi}{\partial z^2} = 0 \tag{8}$$

At the surface of the ground the flow streamlines are tangent to the surface; therefore, at the ground

$$\frac{u_\infty + u'}{dx/dt} = \frac{v'}{dy/dt} = \frac{w'}{dz/dt} \tag{9}$$

If the approximations of small perturbation theory (ref. 5) are used,

$$w' = u_\infty \frac{\partial z}{\partial x}$$

at the surface of the ground $(z = h)$ which gives the boundary condition for φ as

$$\frac{\partial \varphi}{\partial z} = u_\infty \frac{\partial h}{\partial x} \tag{10}$$

For small perturbation theory, a Taylor expansion of quantities away from the base plane $z = 0$ shows that to a first-order approximation the boundary condition can be applied at the base plane $z = 0$. Hence, the boundary condition for equation (8) becomes

$$\left. \frac{\partial \varphi}{\partial z} \right|_{z=0} = u_\infty \frac{\partial h}{\partial x} \tag{11}$$

where h is the local terrain height.

4

Superposition of Ridges to Obtain Velocities for Circular and Oval Hills

Flow normal to a two-dimensional ridge. - For flow across a two-dimensional ridge as shown in figure 1 a solution for φ can be tried in the form of a product solution

$$\varphi = u_\infty f(x)e^{-kz} \tag{12}$$

where $k \geq 0$ as the perturbation would not increase with height above the ground. Substituting equation (12) into equation (8) gives the equation for $f(x)$,

$$\frac{d^2f}{dx^2} + k^2f = 0 \tag{13}$$

which has the general solution

$$f = A \sin kx + B \cos kx$$

Then, from equation (12)

$$\varphi = u_\infty(A \sin kx + B \cos kx)e^{-kz}$$

Since this is valid for any $k \geq 0$, the solutions can be superposed to give

$$\varphi = u_\infty \int_{k=0}^{\infty} \left[A(k)\sin kx + B(k)\cos kx\right] e^{-kz} \, dk \tag{14}$$

Then by differentiating

$$u' = \frac{\partial\varphi}{\partial x} = u_\infty \int_{k=0}^{\infty} k\left[A(k)\cos kx - B(k)\sin kx\right] e^{-kz} \, dk \tag{15a}$$

$$w' = \frac{\partial\varphi}{\partial z} = u_\infty \int_{k=0}^{\infty} (-k)\left[A(k)\sin kx + B(k)\cos kx\right] e^{-kz} \, dk \tag{15b}$$

To obtain the equations of the streamlines, equations (15) are substituted into equation (9) to yield

5

$$dz \left\{ 1 + \int_{k=0}^{\infty} k[A(k)\cos kx - B(k)\sin kx] e^{-kz} dk \right\} =$$

$$dx \int_{k=0}^{\infty} (-k)[A(k)\sin kx + B(k)\cos kx] e^{-kz} dk$$

This can be integrated to obtain along any streamline

$$z = \int_{k=0}^{\infty} [A(k)\cos kx - B(k)\sin kx] e^{-kz} dk + z_0 \tag{16}$$

where z_0 has a different constant value along each streamline.

To evaluate the coefficients $A(k)$ and $B(k)$ the small perturbation approximation that the boundary condition at the surface of the ground can be applied at the base plane $z = 0$ is used. The perturbation theory requires that the ground contour be smooth so that the effect of higher harmonics (large k) is small. Then if $z_0 = 0$ is allowed to correspond to the ground streamline, equation (16) yields

$$h(x) = \int_{k=0}^{\infty} [A(k)\cos kx - B(k)\sin kx] dk$$

For a specified $h(x)$ the $A(k)$ and $B(k)$ can be found by expanding $h(x)$ in a Fourier integral (ref. 8):

$$\left. \begin{array}{l} A(k) = \dfrac{1}{\pi} \displaystyle\int_{\xi=-\infty}^{\infty} h(\xi)\cos k\xi \ d\xi \\[4mm] B(k) = -\dfrac{1}{\pi} \displaystyle\int_{\xi=-\infty}^{\infty} h(\xi)\sin k\xi \ d\xi \end{array} \right\} \tag{17}$$

If the same approximation of referring the ground surface to the base plane is used, equations (15) yield for a distance δ above the ground

$$u = u_{\infty} \left\{ 1 + \int_{0}^{\infty} k[A(k)\cos kx - B(k)\sin kx] e^{-k\delta} dk \right\} \tag{18a}$$

$$w = -u_\infty \int_0^\infty k\left[A(k)\sin kx + B(k)\cos kx\right] e^{-k\delta} \, dk \tag{18b}$$

Now consider a characteristic ridge contour that has been used in the literature (refs. 6 and 7):

$$\frac{h(x)}{h_m} = \frac{1}{1 + \left(\dfrac{x}{b}\right)^2} = \frac{1}{1 + \left(\dfrac{x}{h_m}\right)^2 \left(\dfrac{h_m}{b}\right)^2} \tag{19}$$

where b is the value of x at the half-height of the ridge (fig. 1). The h(x) is an even function, so from equation (17) B(k) = 0, and the integration for A(k) yields

$$A(k) = h_m b \, e^{-kb} \tag{20}$$

Then from equation (18a) the u becomes

$$\frac{u}{u_\infty} = 1 + h_m b \int_{k=0}^\infty k \, e^{-(b+\delta)k} \cos kx \, dk$$

which integrates to

$$\frac{u}{u_\infty} = 1 + h_m b \left\{ \frac{(b + \delta)^2 - x^2}{\left[(b + \delta)^2 + x^2\right]^2} \right\} \tag{21}$$

At the peak of the ridge x = 0, and at height δ above the peak the velocity is

$$\frac{u}{u_\infty} = 1 + \frac{h_m}{b} \frac{1}{\left(1 + \dfrac{\delta}{b}\right)^2} \tag{22}$$

Undisturbed flow at an angle to two-dimensional ridge. - In figure 1 the centerline of the ridge was along the y-axis; now let it be at an angle γ to the y-axis as shown in figure 2. If equation (19) is used, the height of the ridge at location (r, θ) is

7

$$\frac{h(r, \theta)}{h_m} = \frac{1}{1 + \left(\frac{\xi}{b}\right)^2} = \frac{1}{1 + \left(\frac{r}{b}\right)^2 \cos^2(\theta + \gamma)}$$

The undisturbed velocity u_∞ has a component $u_\infty \sin \gamma$ parallel to the ridge that is unchanged by the ridge. The component $u_\infty \cos \gamma$ normal to the ridge is influenced by the ridge as given by equation (21). Then at (r, θ), adding the components in the x-direction gives

$$u(r, \theta) = (u_\infty \sin \gamma)\sin \gamma + u_\infty \cos \gamma \left(1 + h_m b \left\{\frac{(b + \delta)^2 - \xi^2}{\left[(b + \delta)^2 + \xi^2\right]^2}\right\}\right) \cos \gamma$$

Substituting for ξ yields

$$u(r, \theta) = u_\infty \sin^2\gamma + u_\infty \cos^2\gamma \left(1 + h_m b \left\{\frac{(b + \delta)^2 - r^2 \cos^2(\theta + \gamma)}{\left[(b + \delta)^2 + r^2 \cos^2(\theta + \gamma)\right]^2}\right\}\right)$$

which simplifies to

$$\frac{u(r, \theta)}{u_\infty} = 1 + h_m b \cos^2\gamma \left\{\frac{(b + \delta)^2 - r^2 \cos^2(\theta + \gamma)}{\left[(b + \delta)^2 + r^2 \cos^2(\theta + \gamma)\right]^2}\right\} \tag{24}$$

Flow across an oval mound. - Consider an oval mound as in figure 3 with its major axis at an angle ω to the y-axis as shown. As discussed in reference 7 a superposition of solutions for two-dimensional ridges at various γ angles can be used to build up the solution for an oval mound. The oval shape is obtained by introducing an angular weighting factor $\Phi(\gamma, \omega)$ into the superposition. The height of the mound is found by using equation (23) as

$$\frac{h(r, \theta)}{h_m} = \frac{\int_{\gamma=-(\pi/2)}^{\pi/2} \Phi(\gamma, \omega) \dfrac{1}{1 + \left(\frac{r}{b}\right)^2 \cos^2(\theta + \gamma)} d\gamma}{\int_{\gamma=-(\pi/2)}^{\pi/2} \Phi(\gamma, \omega) d\gamma} \tag{25}$$

8

A typical weighting function is

$$\Phi(\gamma, \omega) = \cos\left(\left|\frac{2\alpha}{\pi}\right|^{1/3} \frac{\pi}{2}\right)$$

(26)

where

$$\alpha = \gamma - \omega - \pi \qquad \frac{\pi}{2} < (\gamma - \omega)$$

$$\alpha = \gamma - \omega \qquad -\frac{\pi}{2} \le (\gamma - \omega) \le \frac{\pi}{2}$$

$$\alpha = \gamma - \omega + \pi \qquad (\gamma - \omega) < -\frac{\pi}{2}$$

Although the velocity distribution is a function of angle ω, the contour lines of constant ground elevation do not depend on ω. Hence, equation (25) is most conveniently evaluated for $\omega = 0$. This yields

$$\frac{h}{h_m} = \frac{\displaystyle\int_{\gamma=-(\pi/2)}^{\pi/2} \cos\left(\left|\frac{2\gamma}{\pi}\right|^{1/3} \frac{\pi}{2}\right) \frac{d\gamma}{1 + \left(\frac{r}{b}\right)^2 \cos^2(\theta + \gamma)}}{\frac{6}{\pi^2}(\pi^2 - 8)}$$

(27)

Results for the mound height were evaluated by numerical integration for various r/b and θ and will be given later.

The quantity b in equation (27) is the half-width at the half-height of all the component ridges used in the superposition to build up the oval mound contour. The b must now be related to a characteristic dimension of the mound. The characteristic dimension will be taken as r_o, which is in the cross section A-A of the minor axis as shown in figure 3. This would be a known quantity from the hill geometry. Since $\omega = 0$ in equation (27), the locations along section A-A are along the x-axis corresponding to $\theta = 0$. Then, with $h = h_m/2$ and $r = r_o$, equation (27) gives

$$\frac{1}{2} = \frac{\pi^2 \displaystyle\int_{\gamma=-(\pi/2)}^{\pi/2} \cos\left(\left|\frac{2\gamma}{\pi}\right|^{1/3} \frac{\pi}{2}\right) \dfrac{d\gamma}{1 + \left(\dfrac{r_o}{b}\right)^2 \cos^2\gamma}}{6(\pi^2 - 8)} \tag{28}$$

The particular value for r_o/b that satisfies this equation will be given when numerical results are presented. This numerical value fixes the b for a r_o given by the specific hill geometry, and hence is used to relate the results in equation (27) to the physical geometry.

To obtain the flow across a mound having the orientation shown in figure 3, the velocity distribution in equation (24) is superposed by using the same superposition procedure as was used in equation (25). The result is

$$\frac{u(r,\theta)}{u_\infty} = 1 + \frac{h_m b \displaystyle\int_{\gamma=-(\pi/2)}^{\pi/2} \Phi(\gamma,\omega)\cos^2\gamma \left\{\dfrac{(b+\delta)^2 - r^2\cos^2(\theta+\gamma)}{\left[(b+\delta)^2 + r^2\cos^2(\theta+\gamma)\right]^2}\right\} d\gamma}{\displaystyle\int_{\gamma=-(\pi/2)}^{\pi/2} \Phi(\gamma,\omega)\,d\gamma} \tag{29}$$

After substituting equation (26) and integrating the denominator, equation (29) becomes

$$\frac{u(r,\theta)}{u_\infty} = 1 + \frac{\pi^2 h_m b}{6(\pi^2 - 8)} \int_{\gamma=-(\pi/2)}^{\pi/2} \Phi(\gamma,\omega)\cos^2\gamma \left\{\frac{(b+\delta)^2 - r^2\cos^2(\theta+\gamma)}{\left[(b+\delta)^2 + r^2\cos^2(\theta+\gamma)\right]^2}\right\} d\gamma \tag{30}$$

At the top of the mound $r = 0$ and equation (30) becomes

$$\frac{u}{u_\infty} = 1 + \frac{\pi^2 h_m b}{6(\pi^2 - 8)(b + \delta)^2} \frac{1}{\int_{\gamma=-(\pi/2)}^{\pi/2}} \Phi(\gamma, \omega) \cos^2\gamma \, d\gamma$$

$$= 1 + \frac{h_m}{b} \frac{1}{\left(1 + \frac{\delta}{b}\right)^2} \left\{ \frac{\pi^2}{6(\pi^2 - 8)} \int_{\gamma=-(\pi/2)}^{\pi/2} \Phi(\gamma, \omega) \cos^2\gamma \, d\gamma \right\} \tag{31}$$

The integral in equation (31) was evaluated numerically for the Φ given by equation (26): some results for the peak velocity will be given later as a function of the angle of incidence ω of the flow relative to the mound major axis.

Flow across a circular hill. - For the special case of a circular hill (figs. 4 and 5), the weighting function $\Phi = 1$ and equation (25) becomes (note h is now only a function of r)

$$\frac{h(r)}{h_m} = \frac{1}{\pi} \int_{\gamma=-(\pi/2)}^{\pi/2} \frac{d\gamma}{1 + \left(\frac{r}{b}\right)^2 \cos^2(\theta + \gamma)}$$

This is integrated to give

$$\frac{h(r)}{h_m} = \frac{1}{\sqrt{1 + \left(\frac{r}{b}\right)^2}}$$

At $h/h_m = 1/2$, $r \equiv r_o$ so $1/2 = 1 / \sqrt{1 + (r_o/b)^2}$ which gives $b = r_o / \sqrt{3}$. Then the contour of the circular hill is expressed in terms of r_o, which would be known from the hill cross section, as follows:

$$\frac{h(r)}{h_m} = \frac{1}{\sqrt{1 + 3\left(\frac{r}{r_o}\right)^2}} \tag{32}$$

From equation (29) if $\Phi = 1$ and $r = 0$ there is obtained at the top of the axisymmetric hill

$$\frac{u}{u_m} = 1 + \frac{h_m b}{\pi} \frac{1}{(b + \delta)^2} \int_{\gamma = -(\pi/2)}^{\pi/2} \cos^2 \gamma \, d\gamma$$

Integrating and substituting $b = r_0/\sqrt{3}$ give

$$\frac{u}{u_m} = 1 + \frac{\sqrt{3} h_m}{2 r_0} \frac{1}{\left(1 + \sqrt{3} \dfrac{\delta}{r_0}\right)^2} \tag{33}$$

Analysis for Circular (Axisymmetric) Hills by Use of Green's Functions

General relations. - The perturbation potential φ is governed by the Laplace equation (eq. (8)) in the upper half space subject to the boundary condition that the normal derivative of φ be specified at the boundary $z = 0$ as given by equation (11). This is known as the Neumann boundary condition, and the solution for φ can be found from Green's fundamental solution as (ref. 9)

$$\varphi(x, y, z) = -\frac{1}{4\pi} \iint_{\text{x-y plane}} g \frac{\partial \varphi}{\partial \zeta} \, d\xi \, d\eta \tag{34}$$

where g is the Green's function for the Neumann problem. If g (from ref. 10) is inserted, equation (34) becomes

$$\varphi(x, y, z) = -\frac{u_\infty}{2\pi} \int_{\eta = -\infty}^{\infty} \int_{\xi = -\infty}^{\infty} \frac{1}{\left[(\xi - x)^2 + (\eta - y)^2 + z^2\right]^{1/2}} \frac{\partial h}{\partial \xi} \, d\xi \, d\eta \tag{35}$$

Then u' is found by differentiating with respect to x:

$$u' = \frac{\partial \varphi}{\partial x} = -\frac{u_\infty}{2\pi} \int_{\eta = -\infty}^{\infty} \int_{\xi = -\infty}^{\infty} \frac{\xi - x}{\left[(\xi - x)^2 + (\eta - y)^2 + z^2\right]^{3/2}} \frac{\partial h}{\partial \xi} \, d\xi \, d\eta$$

12

A form that is a little more convenient for analytical integration is found by integrating by parts to yield

$$u'(x, y, z) = - \frac{u_\infty}{2\pi} \int_{\eta=-\infty}^{\infty} \int_{\xi=-\infty}^{\infty} \frac{1}{\left[(\xi - x)^2 + (\eta - y)^2 + z^2\right]^{1/2}} \frac{\partial^2 h}{\partial \xi^2} \, d\xi \, d\eta \qquad (36)$$

Of specific interest here is the u-velocity at a distance δ above the peak of the hill (at $x = y = 0$):

$$u'(0, 0, \delta) = - \frac{u_\infty}{2\pi} \int_{\eta=-\infty}^{\infty} \int_{\xi=-\infty}^{\infty} \frac{1}{\left(\xi^2 + \eta^2 + \delta^2\right)^{1/2}} \frac{\partial^2 h}{\partial \xi^2} \, d\xi \, d\eta \qquad (37)$$

Analytical relations for three hill contours. - Solutions will now be found for three different hill contours. To illustrate the Green's function technique in comparison with the previous analysis, the hill contour that was obtained by superposition of ridges will be considered (fig. 5):

$$\frac{h}{h_m} = \frac{1}{\sqrt{1 + 3\left(\frac{r}{r_0}\right)^2}} = \frac{1}{\sqrt{1 + 3\left[\left(\frac{x}{r_0}\right)^2 + \left(\frac{y}{r_0}\right)^2\right]}} \qquad (38)$$

This is differentiated twice with respect to x and then substituted into equation (37). The results are put into polar coordinates to yield

$$\frac{u'(0, 0, \Delta)}{u_\infty} = \frac{3h_m}{2\pi r_0} \int_{R=0}^{\infty} \int_{\theta=0}^{2\pi} \frac{1}{\left(R^2 + \Delta^2\right)^{1/2}} \left[\frac{1}{\left(1 + 3R^2\right)^{3/2}} - \frac{9R^2 \cos^2\theta}{\left(1 + 3R^2\right)^{5/2}}\right] R \, dR \, d\theta$$

Integrating over θ gives

$$\frac{u'(0,0,\Delta)}{u_\infty} = \frac{3h_m}{2\pi r_0} \int_{R=0}^{\infty} \frac{1}{\left(R^2 + \Delta^2\right)^{1/2}} \left[\frac{2\pi}{\left(1 + 3R^2\right)^{3/2}} - \frac{9\pi R^2}{\left(1 + 3R^2\right)^{5/2}} \right] R \, dR$$

If $1 + 3R^2$ is the square of a new variable of integration this can be integrated; the $u = u_\infty + u'$ then becomes

$$\frac{u}{u_\infty} = 1 + \frac{\sqrt{3}}{2} \frac{h_m}{r_0} \frac{1}{\left(1 + \sqrt{3} \dfrac{\delta}{r_0}\right)^2} \tag{39}$$

This is in agreement with equation (33).

A second circular hill contour that will be considered is

$$\frac{h}{h_m} = \frac{1}{1 + \left(\dfrac{r}{r_0}\right)^2} = \frac{1}{1 + \left(\dfrac{x}{r_0}\right)^2 + \left(\dfrac{y}{r_0}\right)^2} \tag{40}$$

This is of interest because it has the same profile that was used for the two-dimensional ridge (eq. (19)), and the results using equation (40) will provide a comparison between the flow acceleration effects by a two-dimensional ridge and a circular hill having the same contour.

Equation (40) is differentiated twice with respect to x, and the results are substituted into equation (37). After putting the results into polar coordinates the velocity perturbation above the peak of the hill is given by

$$\frac{u'(0,0,\Delta)}{u_\infty} = \frac{h_m}{\pi r_0} \int_{R=0}^{\infty} \int_{\theta=0}^{2\pi} \frac{1}{\left(R^2 + \Delta^2\right)^{1/2}} \left[\frac{1}{\left(1 + R^2\right)^2} - \frac{4R^2 \cos^2\theta}{\left(1 + R^2\right)^3} \right] R \, dR \, d\theta$$

Integrating over θ gives

$$\frac{u'(0,0,\Delta)}{u_\infty} = \frac{h_m}{\pi r_o} \int_{R=0}^{\infty} \frac{1}{\left(R^2 + \Delta^2\right)^{1/2}} \left[\frac{2\pi}{\left(1 + R^2\right)^2} - \frac{4\pi R^2}{\left(1 + R^2\right)^3} \right] R \; dR$$

If $R^2 + \Delta^2$ equals the square of a new variable of integration, the previous equation can be integrated to yield

$$\frac{u(0,0,\delta)}{u_\infty} = 1 + \frac{2h_m}{r_o} \left\{ \left[\frac{r_o^5 + 2r_o^3 \delta^2}{4\left(r_o^2 - \delta^2\right)^{5/2}} \right] \left[\cos^{-1}\left(\frac{\delta}{r_o}\right) \right] - \frac{3\delta r_o^3}{4\left(r_o^2 - \delta^2\right)^2} \right\} \tag{41}$$

As a third example to determine the effect of hill contour, the following exponential shape will be examined (see fig. 5):

$$\frac{h}{h_m} = \exp\left[-\beta^2 \left(\frac{r}{r_o}\right)^2 \right] \tag{42}$$

where $\beta^2 = \ln 2 = 0.693$. Substituting into equation (37) yields, after placing the results in dimensionless polar coordinates,

$$\frac{u'(0,0,\Delta)}{u_\infty} = \frac{\beta^2 h_m}{\pi r_o} \int_{R=0}^{\infty} \int_{\theta=0}^{2\pi} \frac{1}{\left(R^2 + \Delta^2\right)^{1/2}} \left(e^{-\beta^2 R^2} - 2\beta^2 R^2 \cos^2\theta \; e^{-\beta^2 R^2} \right) R \; dR \; d\theta$$

In a similar fashion to what was done for the previous two contours, this is integrated to yield

$$\frac{u(0,0,\delta)}{u_\infty} = 1 + 2\beta \frac{h_m}{r_o} \left\{ -\frac{1}{2}\beta\frac{\delta}{r_o} + \frac{\sqrt{\pi}}{2} e^{(\beta\delta/r_o)^2} \left[\frac{1}{2} + \left(\frac{\beta\delta}{r_o}\right)^2 \right] \left[1 - \text{erf}\left(\frac{\beta\delta}{r_o}\right) \right] \right\} \tag{43}$$

Some results from these relations will be given later.

Superposition of the Effect of Two Hills

In figure 6 two hills are shown, and a quantity of interest is the velocity augmentation at the notch between the hills. The flow direction is normal to the line between the hill centers. Since the Laplace equation for the perturbation potential is linear, the perturbation potential for two hills can be found by adding the potentials for each of the individual hills:

$$u = \frac{\partial}{\partial x}(u_\infty x + \varphi_1 + \varphi_2) = u_\infty + u_1' + u_2' \tag{44}$$

Within the assumptions of small perturbation theory the surface of the combination of two hills is taken to be at the base plane (z = 0) as was the case for a single hill. Then to obtain the perturbation at the location of interest (point N) in figure 6, the u' is obtained at z = 0 for a single hill at a radius m/2 in the plane normal to the direction of the flow. From equation (29) with r = m/2, $\theta = \pi/2$, and $\delta = 0$, this is

$$\frac{u'}{u_\infty} = \frac{h_m b}{\pi} \int_{-(\pi/2)}^{\pi/2} \left\{ \frac{b^2 - \left(\frac{m}{2}\right)^2 \cos^2\left(\frac{\pi}{2} + \gamma\right)}{\left[b^2 + \left(\frac{m}{2}\right)^2 \cos^2\left(\frac{\pi}{2} + \gamma\right)\right]^2} \right\} \cos^2\gamma \, d\gamma$$

Using $\cos\left[(\pi/2) + \gamma\right] = -\sin\gamma$ and adding the effect of the two perturbations give at point N

$$\frac{u}{u_\infty} = 1 + \frac{h_m}{b}\frac{2}{\pi} \int_{-(\pi/2)}^{\pi/2} \left\{ \frac{1 - \left(\frac{m}{2b}\right)^2 \sin^2\gamma}{\left[1 + \left(\frac{m}{2b}\right)^2 \sin^2\gamma\right]^2} \right\} \cos^2\gamma \, d\gamma$$

For a single hill for which equation (29) is valid there was obtained $b = r_0/\sqrt{3}$ so that

$$\frac{u}{u_\infty} = 1 + \frac{\sqrt{3}h_m}{r_o}\left[\frac{2}{\pi}\int_{-(\pi/2)}^{\pi/2}\left\{\frac{1 - \frac{3}{4}\left(\frac{m}{r_o}\right)^2\sin^2\gamma}{\left[1 + \frac{3}{4}\left(\frac{m}{r_o}\right)^2\sin^2\gamma\right]^2}\right\}\cos^2\gamma\ d\gamma\right] \tag{45}$$

The perturbation velocity can then be written as

$$\frac{u'}{u_\infty}\frac{r_o}{h_m} = \sqrt{3}\left[I\left(\frac{m}{r_o}\right)\right] \tag{46}$$

The quantity $I(m/r_o)$ was calculated numerically and results for $(u'/u_\infty)(r_o/h_m)$ will be given later.

As a second example to show the effect of superposing two hills, results will be calculated for two adjacent exponential hills as described by equation (42). At the ground, $z = 0$, equation (36) gives the velocity perturbation as

$$u'(x, y, 0) = -\frac{u_\infty}{2\pi}\int_{\eta=-\infty}^{\infty}\int_{\xi=-\infty}^{\infty}\frac{1}{\left[(\xi - x)^2 + (\eta - y)^2\right]^{1/2}}\frac{\partial^2 h}{\partial\xi^2}\ d\xi\ d\eta$$

From equation (42)

$$\frac{h}{h_m} = e^{-\beta^2(r/r_o)^2} = e^{-\left(\beta^2/r_o^2\right)(x^2+y^2)}$$

so that

$$\frac{\partial^2 h}{\partial x^2} = -2h_m\frac{\beta^2}{r_o^2}e^{-\left(\beta^2/r_o^2\right)(x^2+y^2)}\left(1 - 2\beta^2\frac{x^2}{r_o^2}\right)$$

Let $\hat{h} = \beta h/r_o$, $\hat{\xi} = \beta\xi/r_o$, etc.; the velocity perturbation then becomes

$$\frac{u'}{u_\infty} = \frac{\hat{h}_m}{\pi} \int_{\hat{\eta}=-\infty}^{\infty} \int_{\hat{\xi}=-\infty}^{\infty} \frac{1}{\left[(\hat{\xi} - \hat{x})^2 + (\hat{\eta} - \hat{y})^2\right]^{1/2}} \, e^{-(\hat{\xi}^2 + \hat{\eta}^2)}(1 - 2\hat{\xi}^2)d\hat{\xi} \, d\hat{\eta}$$

As shown in figure 6, the locations of interest for use in the superposition of two hills are along the y-axis (x = 0) which gives

$$\frac{u'(x=0, y)}{u_\infty} = \frac{\hat{h}_m}{\pi} \int_{-\infty}^{\infty} \int_{-\infty}^{\infty} \frac{1}{\left(\hat{\xi}^2 + \hat{\eta}^2 - 2\hat{\eta}\hat{y} + \hat{y}^2\right)^{1/2}} \, e^{-(\hat{\xi}^2 + \hat{\eta}^2)}(1 - 2\hat{\xi}^2)d\hat{\xi} \, d\hat{\eta}$$

Transforming to polar coordinates gives

$$\frac{u'(y)}{u_\infty} = \frac{\hat{h}_m}{\pi} \int_{R=0}^{\infty} \int_{\theta=0}^{2\pi} \frac{1}{\left(R^2 - 2\hat{y}R \sin\theta + \hat{y}^2\right)^{1/2}} (1 - 2R^2 \cos^2\theta)e^{-R^2} R \, dR \, d\theta \tag{47}$$

If the double integral is given by $\pi G(\hat{y})$, this is written as

$$\frac{u'}{u_\infty} \frac{r_o}{h_m} = \beta G(\hat{y}) \tag{48}$$

The analytical evaluation of $G(\hat{y})$ is given in appendix B.

To superpose the effect of two hills the location of interest is at $y = m/2$ $\left[\hat{y} = (\beta/2)(m/r_o)\right]$. Then at the notch between the two hills equation (44) yields

$$\frac{u}{u_\infty} = 1 + 2\beta \frac{h_m}{r_o} G\left(\frac{\beta}{2} \frac{m}{r_o}\right)$$

An expression for G along with numerical values will be given in appendix B, and the velocity perturbation will be plotted in the form

18

$$\frac{u'}{u_\infty} \frac{r_0}{h_m} = 2\beta G\left(\frac{\beta}{2} \frac{m}{r_0}\right) \tag{49}$$

RESULTS AND DISCUSSION

Flow Across a Ridge

The contour of the ridge as given by equation (19) is plotted in figure 7 for a few different values of h_m/b, the ratio of maximum height to the half-width of the ridge at half-height. From equation (22) the surface velocity at the peak of the hill is

$$\frac{u}{u_\infty} = 1 + \frac{h_m}{b}$$

so that the most gradual of the three ridges in figure 7 will give $u/u_\infty = 1.33$ at the peak. For the most steep ridge shown, $u/u_\infty = 2$ at the peak of the ridge, and since the velocity perturbation is not small the accuracy is questionable. The accuracy is probably satisfactory for the two other ridges shown with $h_m/b = 1/2$ and $1/3$.

Flow Across a Circular Hill

The contours of three different circular hills are shown in figure 5 for $h_m/r_0 = 0.5$. From equations (39), (41), and (43) the surface velocity at the peak of these hills is

$$\frac{u}{u_\infty} = 1 + C\frac{h_m}{r_0}$$

where the coefficient C is given in the following table for various hill contours:

Hill contour, h/h_m	Coefficient, C
$\dfrac{1}{\sqrt{1+3\left(\dfrac{r}{r_o}\right)^2}}$	$\dfrac{\sqrt{3}}{2} = 0.866$
$\dfrac{1}{1+\left(\dfrac{r}{r_o}\right)^2}$	$\dfrac{\pi}{4} = 0.785$
$\exp\left[-(\ln 2)\left(\dfrac{r}{r_o}\right)^2\right]$	$\dfrac{\sqrt{\pi \ln 2}}{2} = 0.738$

The largest C, which provides the largest velocity increase, corresponds to the profile with the steepest contour near the peak. For the contours shown in figure 5 where $h_m/r_o = 0.5$, the velocities at the peak are 1.37 to 1.43 times the undisturbed free stream velocity. Since these perturbations are not small compared to 1 the question arises as to whether results from small perturbation theory are meaningful for hills with h_m/r_o this large. To obtain an indication of the error, a rough comparison can be made with results for flow over ellipsoids (ref. 11). These results indicate that the small perturbation theory is in error only about 5 percent for $h/r_o = 1/3$, so the error for $h/r_o = 1/2$ is probably acceptable. For $h_m/r_o < 1/4$ the theory should be quite accurate.

The second contour in the table of C values is the same as the contour of the two-dimensional ridge considered previously. Comparing with equation (22) shows that at the peak the acceleration by the hill is 78.5 percent of that for the ridge. This difference is the "three-dimensional relief effect" and results from part of the flow going around the hill rather than all passing over the crest of the ridge.

Flow Across an Oval Mound

The local height of an oval mound is given by equation (27) as a function of a dimensionless radial coordinate r/b and angle θ as shown in the inset of figure 8. Contours were obtained by numerical integration of equation (27) and are shown in figure 8 for various angles where $\theta = 0$ corresponds to the cross section across the most narrow part of the mound. From equation (28) the characteristic length r_o is defined as the radius within the cross section $\theta = 0$ at which the mound height is one-half the maximum height. From figure 8 there is obtained (at $\theta = 0$ and $h/h_m = 1/2$) $r_o/b = 1.22$ so

that $b = 0.820\, r_0$. From the size of the actual mound, the r_0 is obtained at the half-height of the most narrow cross section; thus, the value of b is then known. For convenience a second abscissa scale of r/r_0 is given in figure 8. Figure 9 shows the shapes of contours of equal height. The mound is approximately twice as long as it is wide.

From equation (31) the surface velocity at the peak of the mound is

$$\frac{u}{u_\infty} = 1 + \frac{u'}{u_\infty} = 1 + \frac{h_m}{r_0}\left[\frac{1.22\,\pi^2}{6(\pi^2 - 8)}\int_{\varphi=-(\pi/2)}^{\pi/2}\Phi(\gamma, \omega)\cos^2\gamma\; d\gamma\right]$$

The quantity in square brackets, which is equal to $(r_0/h_m)(u'/u_\infty)$, was evaluated numerically and is plotted in figure 10 as a function of the angle ω which specifies the wind direction. When $\omega = 0$ the wind is blowing along the short axis of the mound and this provides the maximum velocity enhancement:

$$\frac{u'}{u_\infty}(\omega = 0) = 0.905\,\frac{h_m}{r_0}$$

As the wind shifts away from the direction along the short axis, the perturbation decreases and reaches a minimum for $\omega = 90^{\circ}$ where

$$\frac{u'}{u_\infty}(\omega = 90^{\circ}) = 0.315\,\frac{h_m}{r_0}$$

The contour for $\theta = 0$ in figure 8 is very close to that for the ridge in figure 7 and the $1/[1 + (r/r_0)^2]$ hill contour in figure 5. The velocity perturbation at the peak of the ridge or hill is in all cases equal to a constant times the maximum height of the ground divided by the horizontal distance to the location of the ridge or hill half-height. The constant is 1 for the ridge, 0.905 for flow parallel to the shorter axis of the oval mound, and 0.785 for the circular hill.

Flow In Notch Between Two Adjacent Hills

A possible location for wind velocity enhancement is at the notch between two hills. This geometry is illustrated in figure 6 and the location of interest is at point N. The wind direction is normal to the line connecting the centers of the two hills. The coordinate l is along this line and extends from the symmetry plane of the combined geom-

etry of the two hills. The cross section A-A in figure 6(b) is given in figures 11(b) and (c) and 12(b) for two hill contours having various spacings apart.

Figure 11 deals with the superposition of hills having the contour

$$\frac{h}{h_m} = \frac{1}{\sqrt{1 + 3\left(\frac{r}{r_o}\right)^2}}$$

Part (a) of the figure shows the hill contour for three values of h_m/r_o. As shown by figure 6, m is the spacing between the hills. Adding the heights of the hills for two different spacings yields parts (b) and (c) of figure 11. These two parts show the cross section A-A as shown in figure 6. Figure 12(a) shows the contours of two single hills having the shape

$$\frac{h}{h_m} = \exp\left[-(\ln 2)\left(\frac{r}{r_o}\right)^2\right]$$

The cross section when two of these hills are superposed is shown in figure 12(b).

For the hill contour in figure 11 the surface velocity perturbation at point N in the notch between the hills is given by $\sqrt{3}$ I where I is the quantity in square brackets in equation (45). This has been evaluated numerically and is plotted in figure 13 as a function of spacing between the hills. For the hills shown in figure 12 the velocity perturbation at the ground midway between the hills is given by equation (49). This has been evaluated in appendix B and is plotted as the dashed line in figure 13.

Figure 13 shows how the velocity perturbation at the notch between the hills diminishes as the spacing between the centers of the two hills is increased. In the vicinity of $r/r_o = 2$ the hill height in figure 12 decreases much more rapidly than for the contour in figure 11. As m/r_o is increased in figure 13, this accounts for the rapid drop in the dashed curve as compared with the solid curve. The results show that for a typical case of hills with $h_m/r_o = 1$ spaced at $m/r_o = 4$ the velocity perturbation is about 20 percent of the undisturbed velocity. For the same spacing, if the hill height is reduced in half so that $h_m/r_o = 1/2$, then the perturbation is reduced to about 10 percent.

CONCLUSIONS

Potential flow solutions have been obtained for wind passing over some forms of ground topography that can provide a localized velocity increase. The geometries studied are axisymmetric hills, an oval hill, a two-dimensional ridge, and the notch between two

circular hills. These are possible terrain features to provide locally increased velocities for windmill siting.

The hills and the ridge have cross sections typical of those found naturally. The characteristic hill or ridge dimensions are the maximum height h_m and the horizontal distance from the center line or center plane to the location of the half-height; this horizontal distance is r_0 for a hill and b for a ridge. A quantity of interest is the velocity perturbation u' at the ground at the peak of the hill or ridge where the maximum velocity increase occurs from the uniform incident velocity. The velocity perturbation was found to equal h_m/b for the ridge shape that was analyzed, and it was equal to about $0.8 h_m/r_0$ for a hill. The coefficient of 0.8 for the hill is an average value, as it depends somewhat on the specific hill shape. A range of 0.74 to 0.87 was found for some typical hill contours. Comparing an axisymmetric hill with a ridge having the same contour showed that the increase of velocity at the peak of the hill was 78.5 percent of that for the ridge. This is the three-dimensional relief effect wherein some of the flow passes around the hill rather than all passing over the crest as is the case for a two-dimensional ridge.

A superposition of ridges was used to obtain the flow over an elongated mound with oval shaped contours of constant height. Calculations were made showing the effect of the flow approaching the mound from various directions relative to the mound major axis. When the flow was along the short dimension of the mound the behavior was close to that across a two-dimensional ridge. A much smaller effect was produced when the flow was along the long axis of the mound. This would be expected as the flow is unaffected when moving parallel to a two-dimensional ridge.

Superposition was used to obtain the velocity increase at the notch between two hills. Increases of 20 percent are possible for hill contours of reasonable shape. Larger increases can be obtained with hills having greater slopes, but these cannot be calculated with the small perturbation theory used here.

Lewis Research Center,
National Aeronautics and Space Administration,
Cleveland, Ohio, September 1, 1976,
506-24.

APPENDIX A

SYMBOLS

A, B	coefficients that are functions of k
b	value of x at half-height of a ridge
G	integral defined by eqs. (47) and (48)
g	Green's function for Neumann problem
h	local height
h_m	maximum height
I	integral defined by eqs. (45) and (46)
k	number ≥ 0
l	coordinate along cross section of two hills (fig. 6)
m	spacing between two hills (fig. 6)
R	dimensionless coordinate, r/r_0
r	radial coordinate
r_0	radial location at which hill is at half-height
t	time
u, v, w	velocity components in x-, y-, z-directions
u', v', w'	velocity component perturbations
u_∞	undisturbed velocity approaching irregular terrain
x, y, z	rectangular coordinates
α	dummy variable in eq. (26)
β^2	constant equal to $\ln 2 = 0.693$
γ	angle of ridge line (fig. 2)
δ	height above peak of hill
Δ	dimensionless coordinate δ/r_0
θ	angular coordinate (see figs. 2 or 3)
ξ	coordinate normal to ridge line (fig. 2)
ξ, η, ζ	dummy variables in the x-, y-, and z-directions
Φ	velocity potential function

φ perturbation velocity potential function

ω angle of major axis of mound (see fig. 3)

Superscript:

^   variable multiplied by β/r_o

APPENDIX B

EVALUATION OF INTEGRAL $G(\hat{y})$[a]

From equation (47) the integral $G(\hat{y})$ is

$$G(\hat{y}) = \frac{1}{\pi} \int_{R=0}^{\infty} \int_{\theta=0}^{2\pi} \frac{(1 - 2R^2 \cos^2\theta)e^{-R^2}}{\left(R^2 - 2\hat{y}R \sin\theta + \hat{y}^2\right)^{1/2}} R \, dR \, d\theta$$

In rectangular coordinates, as given by the relation preceding equation (47), this is equal to

$$G(\hat{y}) = \frac{1}{\pi} \int_{\hat{\eta}=-\infty}^{+\infty} \int_{\hat{\xi}=-\infty}^{+\infty} \frac{(1 - 2\hat{\xi}^2)e^{-(\hat{\xi}^2+\hat{\eta}^2)}}{\left[\hat{\xi}^2 + (\hat{\eta} - \hat{y})^2\right]^{1/2}} \, d\hat{\xi} \, d\hat{\eta}$$

Let a new variable be $\gamma = \hat{\eta} - \hat{y}$ to give

$$G(\hat{y}) = \frac{1}{\pi} \int_{\gamma=-\infty}^{\infty} \int_{\hat{\xi}=-\infty}^{\infty} \frac{(1 - 2\hat{\xi}^2)e^{-[\hat{\xi}^2+(\gamma+\hat{y})^2]}}{\left(\hat{\xi}^2 + \gamma^2\right)^{1/2}} \, d\hat{\xi} \, d\gamma$$

Changing to polar coordinates where $r^2 = \hat{\xi}^2 + \gamma^2$ and $\varphi = \tan^{-1}(\gamma/\hat{\xi})$ yields

$$G(\hat{y}) = \frac{1}{\pi} \int_{r=0}^{\infty} \int_{\varphi=0}^{2\pi} \frac{(1 - 2r^2 \cos^2\varphi)e^{-(r^2+2r\hat{y} \sin\varphi+\hat{y}^2)}}{r} r \, dr \, d\varphi$$

$$= \frac{1}{\pi} \int_{r=0}^{\infty} \int_{\varphi=0}^{2\pi} (1 - 2r^2 \cos^2\varphi)e^{-r^2-\hat{y}^2} e^{-2r\hat{y} \sin\varphi} \, dr \, d\varphi$$

---

[a]This integration was carried out by William F. Ford of NASA, Lewis Research Center.

Since $G(\hat{y}) = G(-\hat{y})$, because the $\sin \varphi$ is integrated over an equal range of positive and negative values, the factor $e^{-2r\hat{y} \sin \varphi}$ can be replaced by $(1/2)(e^{2r\hat{y} \sin \varphi} + e^{-2r\hat{y} \sin \varphi}) = \cosh(2r\hat{y} \sin \varphi) = \cos(2ir\hat{y} \sin \varphi)$ so that $G(\hat{y})$ becomes

$$G(\hat{y}) = \frac{1}{\pi} \int_{r=0}^{\infty} \int_{\varphi=0}^{2\pi} (1 - 2r^2 \cos^2\varphi)e^{-r^2-\hat{y}^2} \cos(2ir\hat{y} \sin \varphi) dr \, d\varphi \qquad (B1)$$

From the definite integral tables (ref. 12, p. 143),

$$\int_{r=0}^{\infty} e^{-r^2} \cos(2ir\hat{y} \sin \varphi) dr = \frac{\sqrt{\pi}}{2} e^{\hat{y}^2 \sin^2\varphi}$$

$$\int_{r=0}^{\infty} 2r^2 \cos^2\varphi \, e^{-r^2} \cos(2ir\hat{y} \sin \varphi) dr = \frac{\sqrt{\pi}}{2} \cos^2\varphi \, e^{\hat{y}^2 \sin^2\varphi} (2\hat{y}^2 \sin^2\varphi + 1)$$

The $G(\hat{y})$ in equation (B1) is then

$$G(\hat{y}) = \frac{1}{2\sqrt{\pi}} \int_{\varphi=0}^{2\pi} e^{-\hat{y}^2 \cos^2\varphi} \sin^2\varphi(1 - 2\hat{y}^2 \cos^2\varphi) d\varphi$$

The double angle formulas are used that $\cos^2\theta = (1/2)(1 + \cos \beta)$ and $\sin^2\theta = (1/2)(1 - \cos \beta)$ where $\beta = 2\theta$ and the $G(\hat{y})$ reduces to

$$G(\hat{y}) = \frac{e^{-(1/2)\hat{y}^2}}{2\sqrt{\pi}} \int_{\beta=0}^{\pi} \left[1 - \cos \beta - \frac{1}{2} \hat{y}^2(1 - \cos 2\beta)\right] e^{-(1/2)\hat{y}^2 \cos \beta} \, d\beta \qquad (B2)$$

From reference 12, page 190, equation (B2) is integrated to give

$$G(\hat{y}) = \frac{e^{-y_0}}{2\sqrt{\pi}} [(1 - y_0)\pi J_0(iy_0) - i\pi J_1(iy_0) - y_0\pi J_2(iy_0)] \qquad (B3)$$

where $y_0 = (1/2)\hat{y}^2$. Using the following identities in equation (B3)

$$J_0(iy_0) = I_0(y_0)$$

$$iJ_1(iy_0) = -I_1(y_0)$$

$$-J_2(iy_0) = I_0(y_0) - \frac{2}{y_0} I_1(y_0)$$

gives $G(\hat{y})$ in the final form

$$G(\hat{y}) = \frac{\sqrt{\pi}}{2} e^{-(1/2)\hat{y}^2} \left[I_0\left(\frac{1}{2}\hat{y}^2\right) - I_1\left(\frac{1}{2}\hat{y}^2\right) \right] \tag{B4}$$

Some values of $G(\hat{y})$ evaluated from equation (B4) are

$\hat{y}$	$G(\hat{y})$	$\hat{y}$	$G(\hat{y})$
0.00	0.886	1.40	0.234
.20	.860	1.60	.166
.40	.787	1.80	.117
.60	.679	2.00	.0826
.80	.556	2.45	.0409
1.00	.433	2.83	.0204
1.20	.324	3.16	.0173

REFERENCES

1. Hino, Mikio: Computer Experiment on Smoke Diffusion Over a Complicated Topography. Atmos. Environ., vol. 2, no. 6, Nov. 1968, pp. 541-558.

2. Leahey, Douglas M.: A Study of Air Flow Over Irregular Terrain. Atmos. Environ., vol. 8, no. 8, Aug. 1974, pp. 783-791.

3. Frenkiel, J.: Wind Profiles Over Hills (In Relation to Wind-Power Utilization). Q. J. Roy. Meteorol. Soc., vol. 88, no. 376, Apr. 1962, pp. 156-169.

4. Sutton, Oliver G.: Micrometeorology. McGraw-Hill Book Co., Inc., 1953.

5. Shapiro, Ascher H.: The Dynamics and Thermodynamics of Compressible Fluid Flow. Vol. 1, The Ronald Press Co., 1953.

6. Scorer, R. S.: Theory of Airflow Over Mountains: III - Airstream Characteristics. Q. J. Roy. Meteorol. Soc., vol. 80, no. 345, July 1954, pp. 417-428.

7. Scorer, R. S.: Airflow Over an Isolated Hill. Q. J. Roy. Meteorol. Soc., vol. 82, no. 351, Jan. 1956, pp. 75-81.

8. Hildebrand, Francis B.: Advanced Calculus for Engineers. Prentice-Hall, Inc., 1949.

9. Morse, Philip M.; and Feshbach, Herman: Methods of Theoretical Physics. Part I. McGraw-Hill Book Co., Inc., 1953, p. 802.

10. Chester, Clive R.: Techniques in Partial Differential Equations. McGraw-Hill Book Co., Inc., 1971, pp. 82-85.

11. Hess, Robert V.; and Gardner, Clifford S.: Study by the Prandtl-Glauert Method of Compressibility Effects and Critical Mach Number for Ellipsoids of Various Aspect Ratios and Thickness Ratios. NACA TN 1792, 1949.

12. Gröbner, Wolfgang; and Hofreiter, Nikolaus: Integral Tables. Part II, Springer-Verlag (Vienna and Innsbruck), 1958.
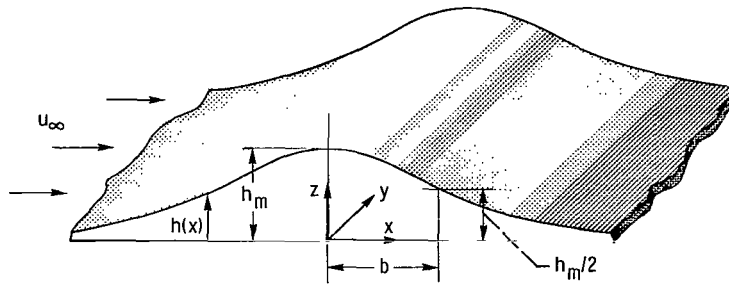
Figure 1. - Two-dimensional ridge with local height $h(x)$ in wind with uniform velocity u_∞.
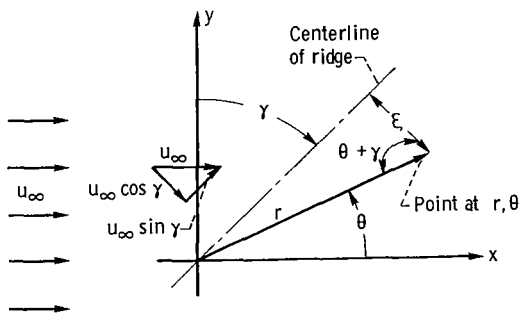
Figure 2. - Coordinates looking down on two-dimensional ridge at an angle to the wind.
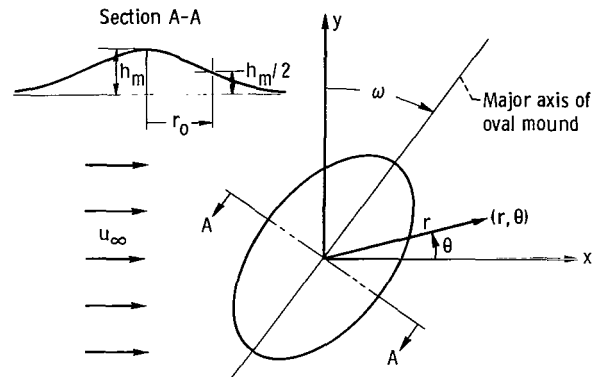
Figure 3. - Coordinates viewing oval mound from above, and geometry of cross section along minor axis of mound.
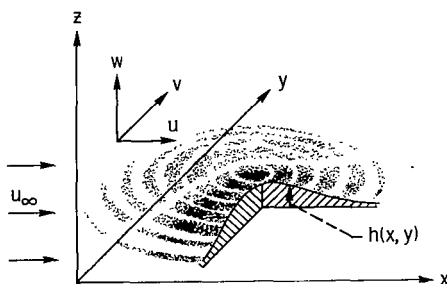
Figure 4. - Circular hill having local height $h(x, y)$ in wind with uniform incident velocity, u_∞.
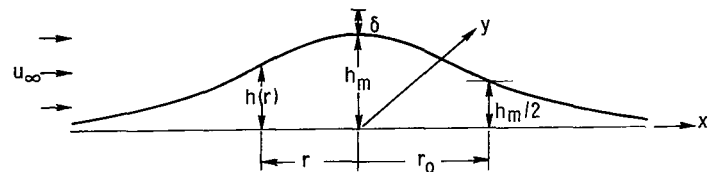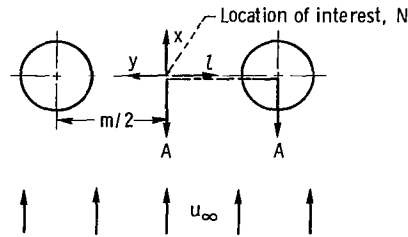

(a) Hill contour showing geometric quantities.

h/h_m

$(1 + 3R^2)^{-1/2}$

$(1 + R^2)^{-1}$

$\exp(-0.693 R^2)$

$R = r/r_0$
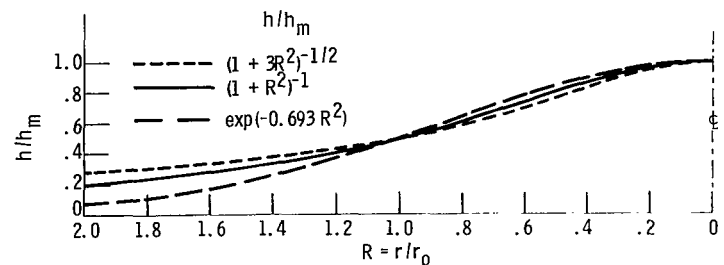
(b) Three different hill contours, $h_m/r_0 = 0.5$.

Figure 5. - Geometry for circular hill.
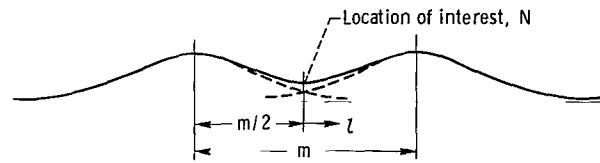
(a) Cross section normal to flow.

(b) Coordinates looking down on hills.

Figure 6. – Geometry for flow across two superposed hills.
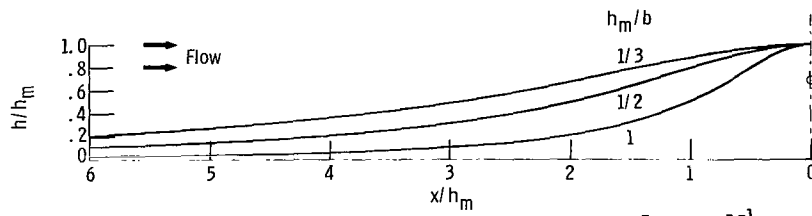
Figure 7. – Contours of two-dimensional ridge, $h(x)/h_m = \left[1 + (x/b)^2\right]^{-1}$.
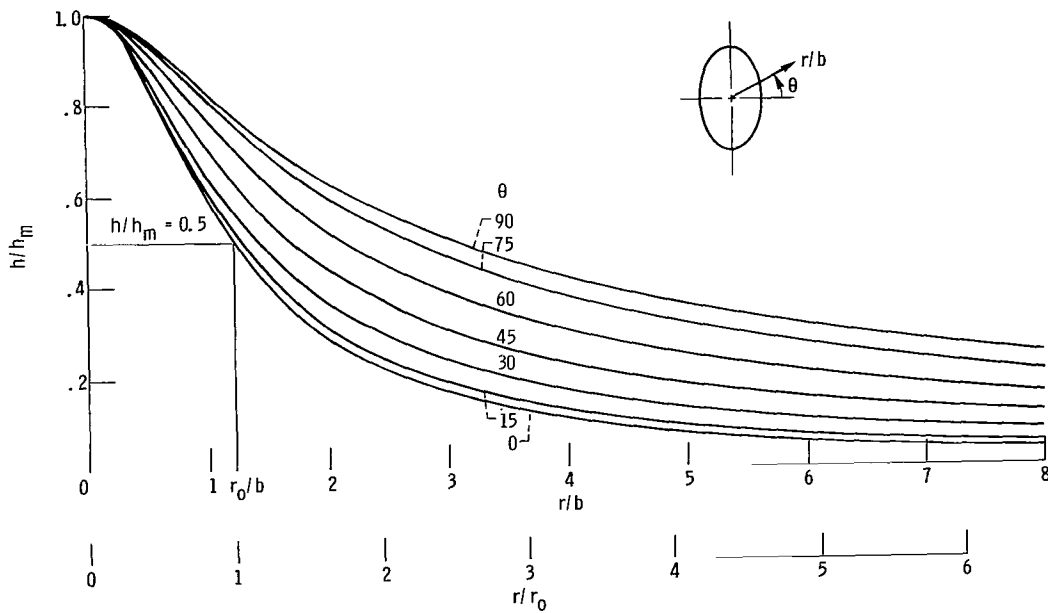
Figure 8. – Height contours of oval mound along radial directions at various angles from the minor axis.
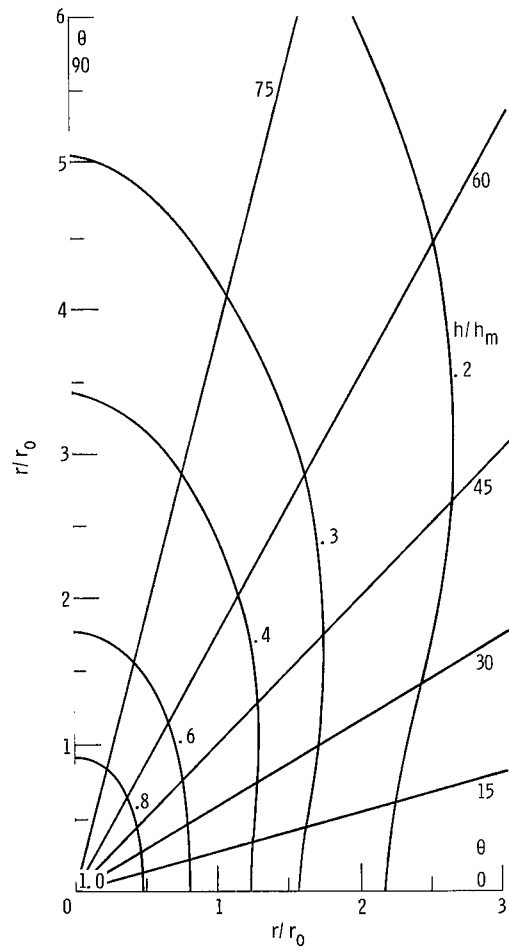
Figure 9. - Contours of constant height for oval mound.
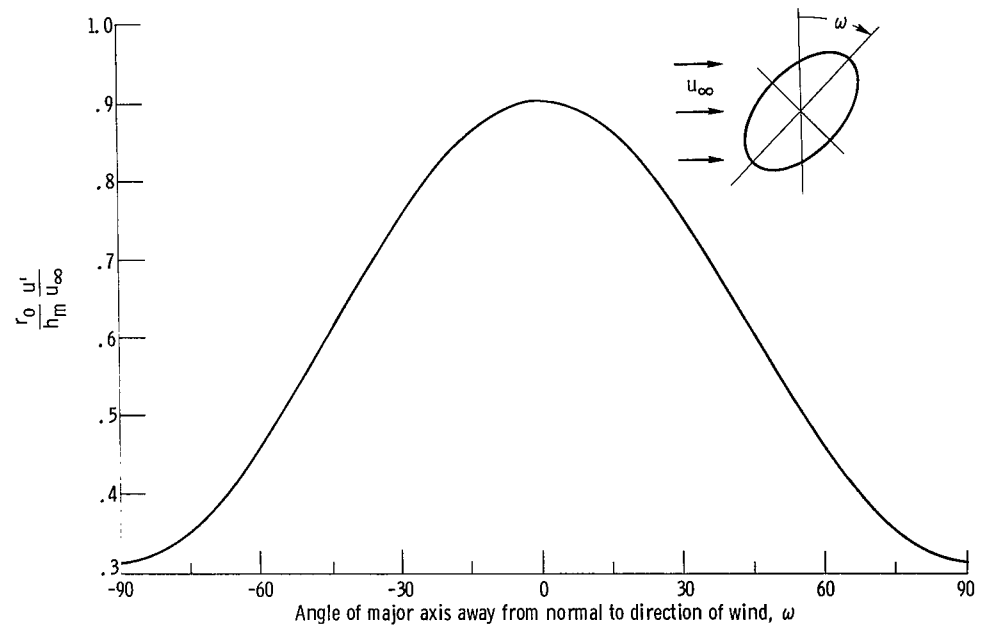
Figure 10. - Velocity perturbation above peak of oval mound for mound at various angles to wind.
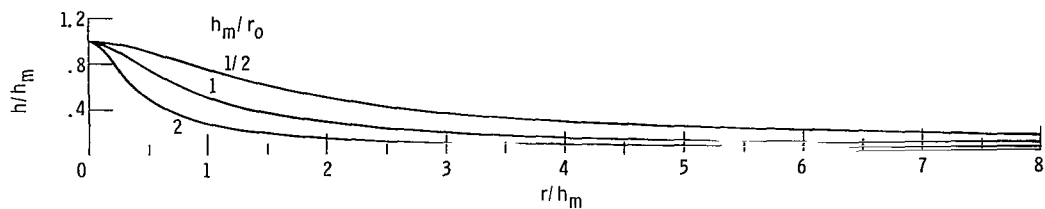
(a) Contours of single hills.
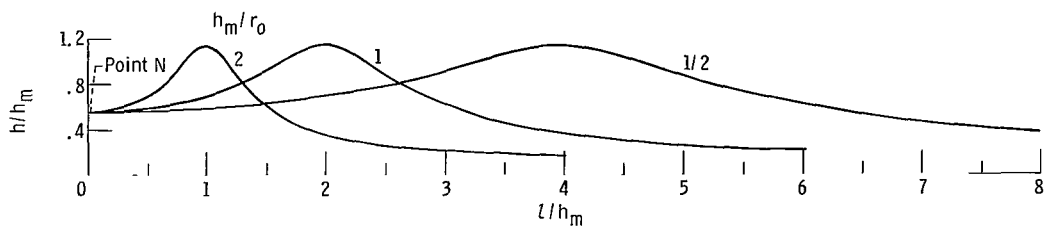
(b) Superposition of two hills, $m/r_0 = 4$.
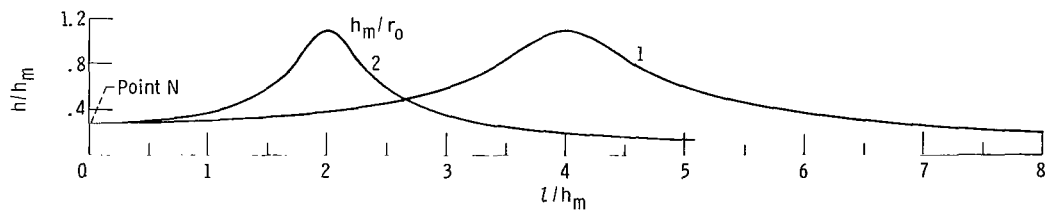
(c) Superposition of two hills, $m/r_0 = 8$.

Figure 11. – Superposition of two hills each having contour $h/h_m = \left[1 + 3(r/r_0)^2\right]^{-1/2}$.
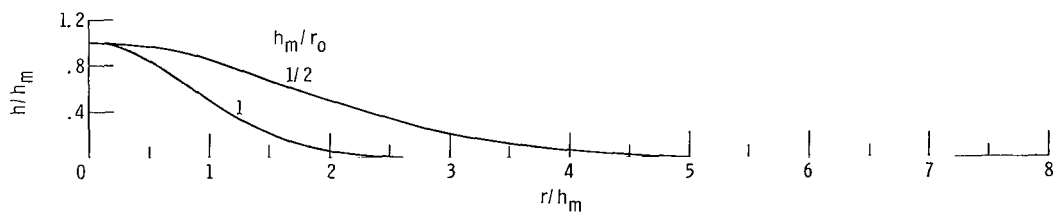
(a) Contours of single hills.
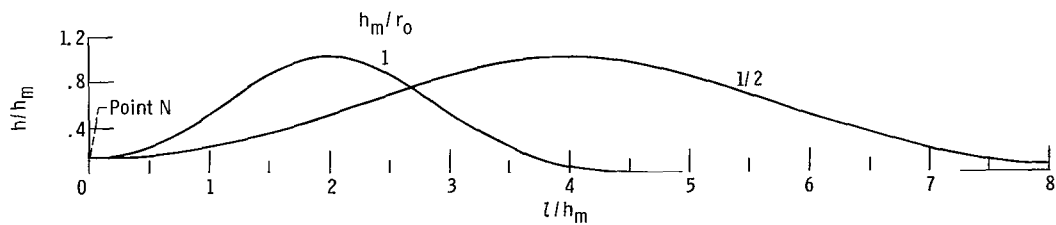
(b) Superposition of two hills, $m/r_0 = 4$.

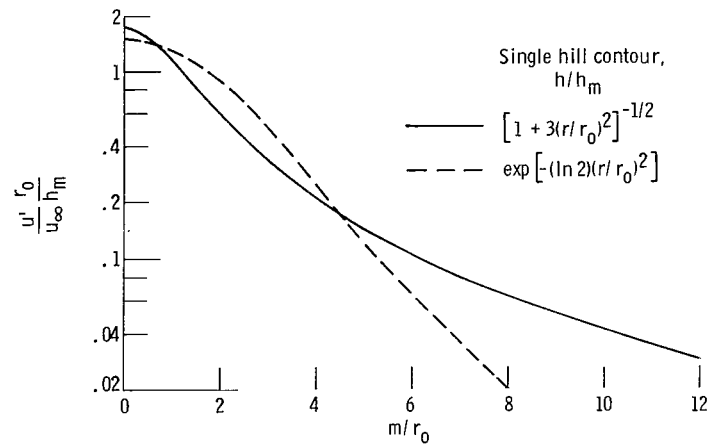Figure 12. – Superposition of two hills each having contour $h/h_m = \exp\left[-(\ln 2)(r/r_0)^2\right]$.

33

Figure 13. – Velocity perturbation at ground at notch midway between two circular hills as function of spacing between hills.

"The aeronautical and space activities of the United States shall be conducted so as to contribute . . . to the expansion of human knowledge of phenomena in the atmosphere and space. The Administration shall provide for the widest practicable and appropriate dissemination of information concerning its activities and the results thereof."
—NATIONAL AERONAUTICS AND SPACE ACT OF 1958

NASA SCIENTIFIC AND TECHNICAL PUBLICATIONS

TECHNICAL REPORTS: Scientific and technical information considered important, complete, and a lasting contribution to existing knowledge.

TECHNICAL NOTES: Information less broad in scope but nevertheless of importance as a contribution to existing knowledge.

TECHNICAL MEMORANDUMS: Information receiving limited distribution because of preliminary data, security classification, or other reasons. Also includes conference proceedings with either limited or unlimited distribution.

CONTRACTOR REPORTS: Scientific and technical information generated under a NASA contract or grant and considered an important contribution to existing knowledge.

TECHNICAL TRANSLATIONS: Information published in a foreign language considered to merit NASA distribution in English.

SPECIAL PUBLICATIONS: Information derived from or of value to NASA activities. Publications include final reports of major projects, monographs, data compilations, handbooks, sourcebooks, and special bibliographies.

TECHNOLOGY UTILIZATION PUBLICATIONS: Information on technology used by NASA that may be of particular interest in commercial and other non-aerospace applications. Publications include Tech Briefs, Technology Utilization Reports and Technology Surveys.

Details on the availability of these publications may be obtained from:

SCIENTIFIC AND TECHNICAL INFORMATION OFFICE

NATIONAL AERONAUTICS AND SPACE ADMINISTRATION
Washington, D.C. 20546